Journal of Applied Electrochemistry (2006) 36:913–918
DOI 10.1007/s10800-006-9155-6

Electro-catalytic oxidation of methanol on a Ni–Cu alloy in alkaline medium

M. JAFARIAN[1,*], R.B. MOGHADDAM[1], M.G. MAHJANI[1] and F. GOBAL[2]
[1]*Department of Chemistry, K. N. Toosi University of Technology, 15875-4416, Tehran, Iran*
[2]*Faculty of Chemistry, Sharif University of Technology, 11365-9516, Tehran, Iran*
*(*author for correspondence, tel.: + 98-21-2285-35-51, fax: + 98-21-2285-36-50, e-mail: mjafarian@kntu.ac.ir)*

Received 22 December 2005; accepted in revised form 28 April 2006

Key words: electro-catalytic oxidation, methanol, nickel, nickel–copper alloy

Abstract

The electro-catalytic oxidation of methanol on a Ni–Cu alloy (NCA) with atomic ratio of 60/40 having previously undergone 50 potential sweep cycles in the range 0–600 mV vs. (Ag/AgCl) in 1 M NaOH was studied by cyclic voltammetry (CV), chronoamperometry (CA) and impedance spectroscopy (EIS). The electro-oxidation was observed as large anodic peaks both in the anodic and early stages of the cathodic direction of potential sweep around 420 mV vs. (Ag/AgCl). The electro-catalytic surface was at least an order of magnitude superior to a pure nickel electrode for methanol oxidation. The diffusion coefficient and apparent rate constant of methanol oxidation were found to be 2.16×10^{-4} cm^2 s^{-1} and 1979.01 cm^3 mol^{-1} s^{-1}, respectively. EIS studies were employed to unveil the charge transfer rate as well as the electrical characteristics of the catalytic surface. For the electrochemical oxidation of methanol at 5.0 M concentration, charge transfer resistance of nearly 111 Ω was obtained while the resistance of the electro-catalyst layer was ca. 329 Ω.

1. Introduction

Extensive studies have been devoted to the electro-catalytic oxidation of methanol which is of paramount importance in the development of direct methanol fuel cells [1, 2]. Although the study of the apparently complex mechanism of the electrochemical reaction is important and may provide guidance to the design of suitable new catalysts [3–6], the modification of the existing known active surfaces [7–10] can be a promising short-cut. In this regard alloying and underpotential deposition of modifiers onto a catalytic surface [11, 12] have been tried in attempts to reduce the seemingly high overpotential associated with the process as well as to overcome the possible impeding effects of the adsorbed intermediates [13]. A great deal of interest has recently been focused on the use of non-noble transition metals in alkaline media [14–17] where less expensive members, copper and nickel, and their modified surfaces have received special attention [18–20]. Both copper and nickel have been reported to effectively catalyze the electro-oxidation of alcohols [7–10, 16] in general and methanol [21] in particular besides the number of other organics that they electrocatalyze in anodic [22, 23] and cathodic reactions. According to the thermodynamic data, copper does not undergo redox processes in the potential range of nickel's electro-activity [24] and modification of nickel by copper has been shown [25, 26] to enhance its electro-catalytic activity in methanol electro-oxidation. The purpose of the present work is to study the electro-catalytic activity of Ni–Cu alloy (NCA) in alkaline solutions and bring it to the attention of workers in the field of direct methanol fuel cell development.

2. Experimental

Sodium hydroxide, copper, nickel and methanol used in this work were Merck products of analytical grade and used as received. Water was doubly distilled. Alloys of Ni–Cu (NCA) with the atomic ratio of 60/40 were cast in cylindrical form with the circular area of 0.03 cm^2. These were fitted into Teflon and the exposed circular surface was polished subsequently with No. 1000 and 2000 emery papers and 0.05 μm alumina powder to mirror bright and rinsed with distilled water prior to use. Electrochemical studies were carried out in a conventional three electrode cell powered by a model 273A EG&G potentiostat/galvanostat and a model 1255 Solartron frequency response analyser. The system was run by a PC through M270 and M398 commercial softwares. The alloy formed the working electrode its potential monitored against a (Ag, AgCl) standard reference electrode and a Pt wire formed the counter electrode. All studies were carried out at 298 ± 2 K.

3. Results and discussion

Figure 1 presents a typical cyclic voltammogram of NCA recorded after 50 consecutive potential cycles, to guarantee the stability of the pattern, in the range 0–600 mV vs. (Ag/AgCl). Two overlapping and poorly defined anodic peaks at around 320 and 420 mV and a well defined cathodic peak at around 220 mV are the main features. The peaks can be assigned to the redox processes:

$$Ni(OH)_2 + OH^- \leftrightarrow NiOOH + H_2O + e^- \quad (1)$$

where the appearance of two anodic peaks are probably due to the formation of α- and β-phases of NiOOH from the corresponding phases of $Ni(OH)_2$ with the β-phase occurring at higher anodic potentials [27–29]. Both phases give rise to a common cathodic peak in the reducing half cycle. To amplify the argument a number of cyclic voltammograms with the potential sweep reversed between 0.3 and 0.6 V vs. (Ag/AgCl) were recorded, (Figure 2), and it was confirmed that both phases convert to a single reduced state.

Figure 3 compares the electro-catalytic activities of NCA with a pure Ni electrode for methanol electro-oxidation in 1 M NaOH solution. Over 10-fold superior activity is found for NCA over pure Ni. The superior catalytic activity of alloy may be due to the filling of Ni d-band vacancies by Cu electrons. Complete filling occurs at ca. 40% copper composition. In a number of cases [30] this also corresponds to the highest activity due to the diminished tendency of Ni to adsorb reactants too strongly. Figure 4 presents cyclic voltammograms of methanol oxidation recorded at various concentrations of methanol in the range 0–2 M. In all measurements the voltammograms are dominated by

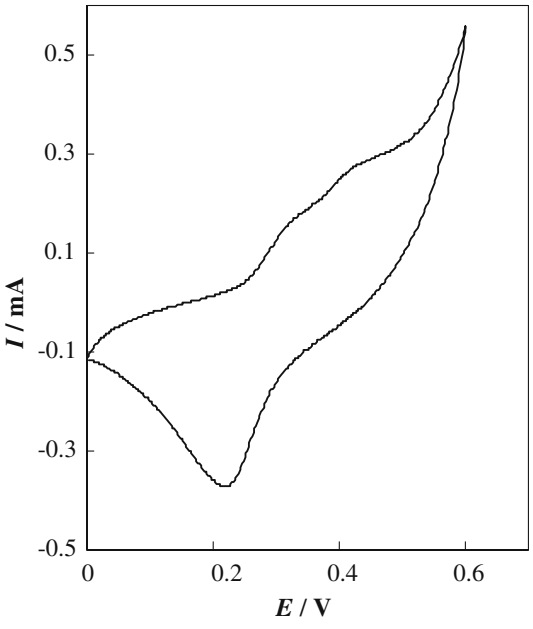

Fig. 1. Cyclic voltammogram of NCA electrode in 1 M NaOH recorded in 50th cycle at a potential sweep rate of 100 mV s^{-1}.

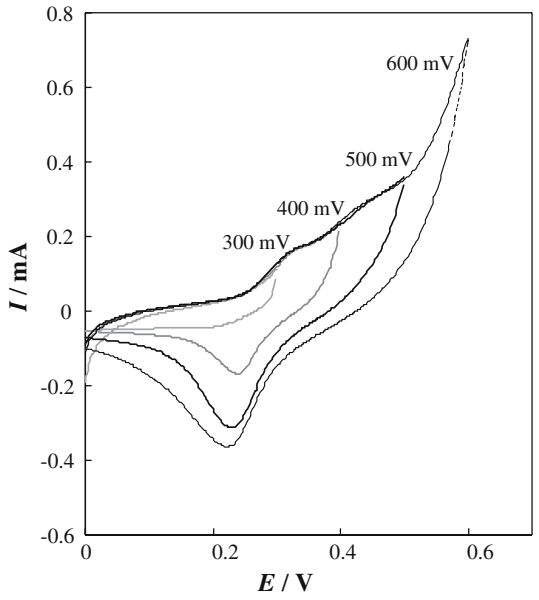

Fig. 2. CVs of NCA electrode at different anodic potential ranges, 0–300, 400, 500 and 600 mV, in 1 M NaOH at potential sweep rate of 100 mV s^{-1}.

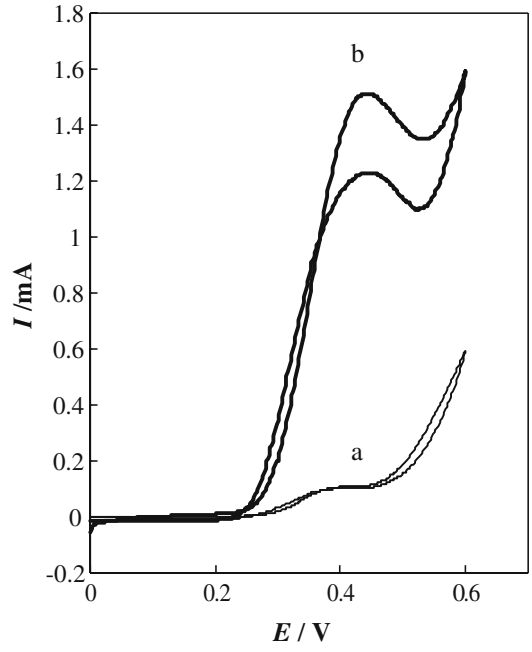

Fig. 3. Cyclic votammogram of smooth nickel electrode (a) and NCA electrode (b) in a solution containing 1 M NaOH and 0.5 M methanol at a potential sweep rate of 10 mV s^{-1}.

large anodic peaks centered around 420 mV vs. (Ag/AgCl) in the anodic half cycle which signify $Ni(OH)_2$/NiOOH mediated electro-oxidation of methanol. The oxidation continues in the early stages of the cathodic half cycle as the adsorbed intermediates are slowly removed and the active sites are regenerated for further adsorption of methanol that are subsequently oxidized due to the still favorable potential [31]. Also, the

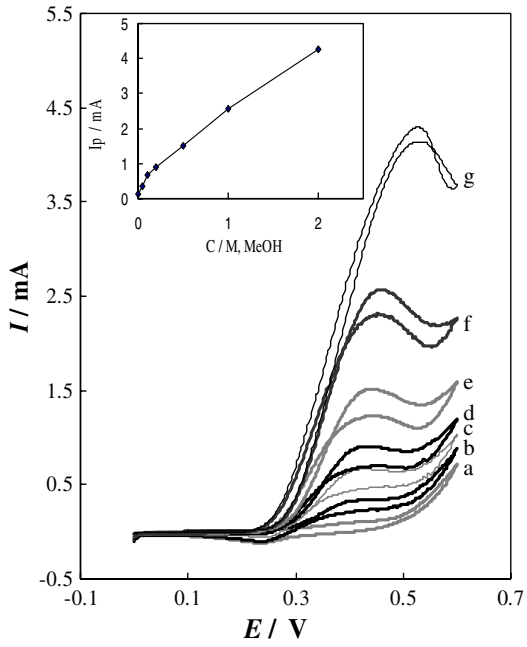

Fig. 4. CVs of NCA electrode in 1 M NaOH at different methanol concentration: 0 (a); 0.05 (b); 0.1 (c); 0.2 (d); 0.5 (e); 1 (f) and 2 M (g) respectively in Potential sweep rate of 10 mV s^{-1}; variation of I_p by methanol concentration (inset).

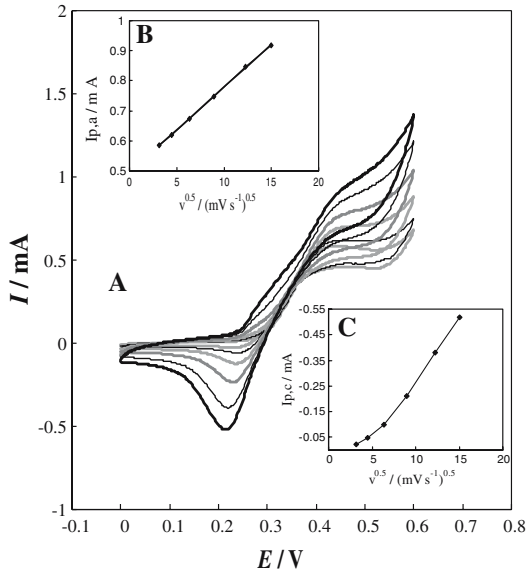

Fig. 5. Typical CVs of NCA electrode in 1 M NaOH and 0.1 M methanol for potential sweep rates of 10, 20, 40, 80, 150 and 225 mV s^{-1} (A), the dependency of anodic peak current (B) and also cathodic peak current at higher potential sweep rates than 40 mV s^{-1} (C) to the square roots of sweep rate.

cathodic peak is dramatically diminished at the low methanol concentration and disappears entirely as its concentration is raised. These observations, along with the fact that methanol is not electro-active in the potential window under consideration, point to the electro-catalytic nature of the phenomenon. Although the slow removal of adsorbed intermediates may contribute to the anodic peak, the origin of the anodic peak is still diffusional as clearly indicated in the linear dependency of the anodic peak current on the square root of the potential sweep rate, (Figure 5A, B). On the other hand, the cathodic peak current depends on the square root of the potential sweep rate only at moderate to high values of the latter, (Figure 5C). This further amplifies the argument on the involvement of NiOOH surface species in the seemingly slow electro-oxidation of methanol. At high potential sweep rates the mentioned species survives and undergoes reduction as the sweep is reversed giving large cathodic peaks, (Figure 5A). Without going into detail, on the basis of this work and the existing literature [32, 33], the following sequence of reactions giving rise to the formation of formate anions is proposed:

$$CH_3OH + Ni(OH)_2 \rightarrow Ni(OH)_2(CH_3OH)_{ads} \quad (2)$$

$$Ni(OH)_2 + OH^- \leftrightarrow NiOOH + H_2O + e^- \quad (3)$$

$$Ni(OH)_2(CH_3OH) + OH^- \rightarrow NiOOH(CH_3OH)_{ads} + H_2O + e^- \quad (4)$$

$$NiOOH(CH_3OH)_{ads} + NiOOH + 2OH^- \rightarrow Ni(OH)_2 + NiOOH(COH)_{ads} + 2H_2O + 2e^- \quad (5)$$

$$NiOOH(COH)_{ads} + OH^- \rightarrow Ni(OH)_2 + HCOO^- \quad (6)$$

while reaction (3) is responsible for the peaks at 320 and 420 mV in the absence of methanol, reaction (4) and (5) generate the peak at 420 mV in the presence of methanol and its increase varies with concentration and probably levels off at concentrations well in excess of 2 M (Figure 4).

To test the stability of the electro-catalyst one hundred potential sweep cycles in the range 0 to 0.6 V were performed in the presence of 0.1 M methanol, (Figure 6). Interestingly enough the catalytic effect seems to be enhanced by a factor of ca. 1.5. Without much speculation the slight increased activity is probably due to the combination of increased surface area (perhaps increased porosity) of the electro-catalytic layer in the course of its repeated building up and tearing down and the increased specific activity due to the slow conversion of α to β-structures. Lower activity of the α-phase is evident in the results presented in Figure 5 where at high potential sweep rates α well resolved shoulder precedes the mediated methanol oxidation peaks. The shoulder presents oxidation of α-$Ni(OH)_2$ to the corresponding NiOOH phase [27–29] which largely survives the anodic half cycle and is reduced along with the surviving β-NiOOH (or generated in the early stages of the cathodic half cycle) in the

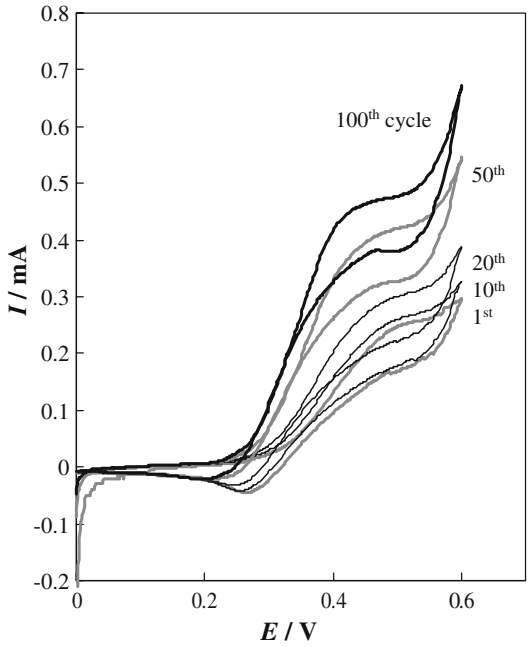

Fig. 6. Presentation of the relative stability of the electro-catalyst in the course of 100 potential sweep cycles; 0.1 M methanol, 10 mV s^{-1} potential sweep rate.

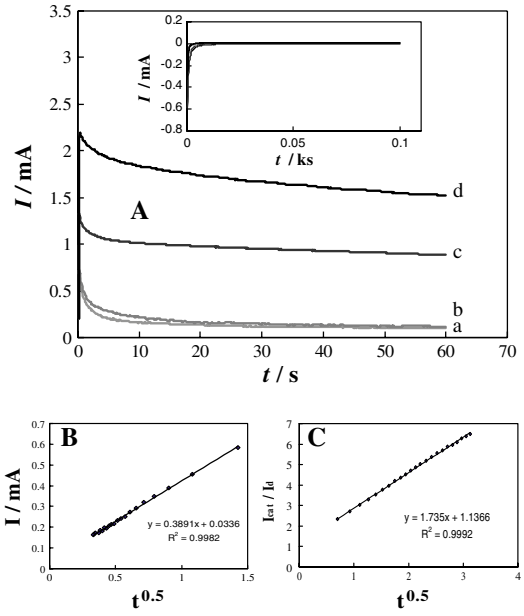

Fig. 7. (A) Chronoamperograms of NCA electrode in 1 M NaOH in the absence (a) and presence of 0.1, 0.5 and 1 M (b, c, d) methanol; potential steps were 420 mV for oxidation, and then 250 mV for reduction (inset), (B) The plot of net current chronoamperogram of NCA in 0.1 M methanol (obtained by subtracting the background current using the point-by-point subtracting method) vs. $t^{-0.5}$. (C) Dependence of I_{cat}/I_d on $t^{0.5}$ derived from the data of chronoamperogram of a and d in part A.

form of a large cathodic peak which also shows slight negative shift in the reducing half cycle.

Chronoamperometry has also been employed to shed more light on the proposed E_rC_i mechanism [34] of the reaction. Figure 7A presents the chronoamperograms in the absence and presence of methanol at various concentrations in 1 M NaOH recorded at 420 mV vs. (Ag/AgCl). The transient current is due to methanol oxidation and varies correspondingly. The dominance of a diffusion controlled process is shown, (Figure 7B), through the I vs. $t^{-0.5}$ linear dependency. From its slope the diffusion coefficient of 2.16×10^{-4} cm^2 s^{-1} was derived (point by point background current removal was employed). Also, the overall rate of methanol oxidation on NCA redox sites can be derived through [34]:

$$I_{cat}/I_d = \lambda^{0.5}[\pi^{0.5}\mathrm{erf}(\lambda^{0.5}) + \exp(-\lambda)/\lambda^{0.5}] \quad (7)$$

where I_{cat} and I_d are currents in the presence and absence of methanol and $\lambda = k' C_m t$ with k', C_m and t the rate constant, bulk methanol concentration and the elapsed time. For $\lambda > 1.5$, $\exp(-\lambda)/\lambda^{0.5}$ is vanishingly small and erf ($\lambda^{0.5}$) approaches unity and equation (7) simplifies to:

$$I_{cat}/I_d = \lambda^{0.5}\pi^{0.5} \quad (8)$$

From the slope of I_{cat}/I_d vs. $t^{0.5}$, (Figure 7C), for 0.5 M methanol solution the value of k' was found to be 1979.01 cm^3 mol^{-1} s^{-1}.

The study of the effect of temperature on the kinetics of methanol electro-oxidation is hampered by the volatility of the substance. A clear increase in the rate with temperature is followed by a decrease due to the evaporation of methanol from the electrochemical cell as the temperature is raised, (Figure 8) and inset.

Figure 9 presents the Nyquist plots recorded at 420 mV dc-offset potential both in the absence (a) and presence (b–g) of various concentrations of methanol

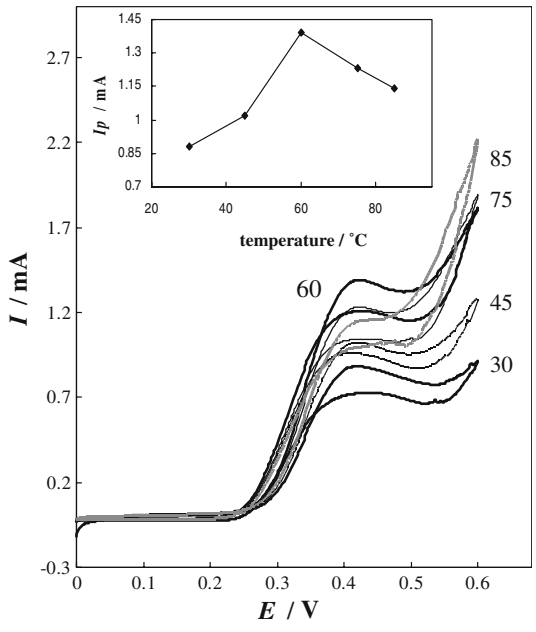

Fig. 8. CVs of NCA in 0.2 M methanol and potential sweep rate of 10 mV s^{-1} using oven temperature of 30, 45, 60, 75 and 85 °C. Dependence of anodic current to temperature values (inset).

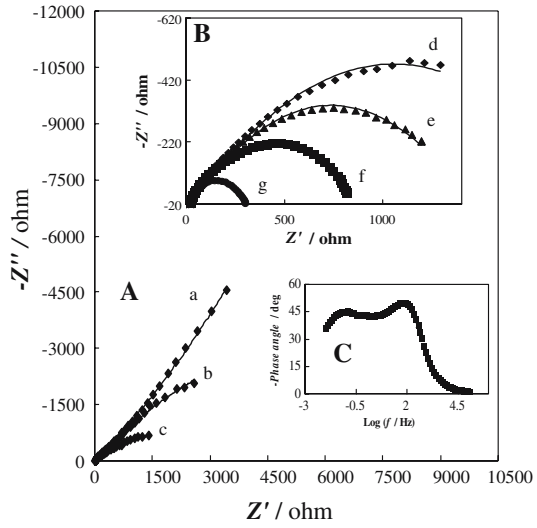

Fig. 9. (A) Nyquist diagrams of NCA electrode in the absence (a) and presence of 0.05 (b), 0.1 (c), (B) 0.2 (d), 0.5 (e), 1 (f) and 5 M (g) methanol in 1 M NaOH medium. DC potential is 420 mV vs. (Ag/AgCl)., (C) Bode profile for 0.1 M methanol, (frequency range is 100 kHz to 10 mHz in all plots).

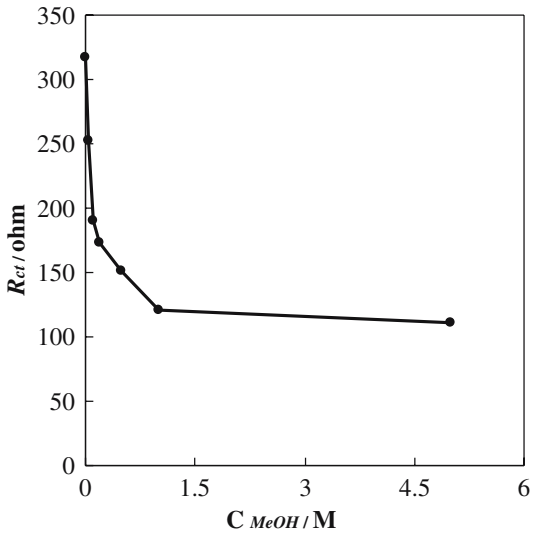

Fig. 10. Dependence of R_{ct} on methanol concentration from the Nyquist diagrams in Fig. 9.

in 1 M NaOH solution. The mechanism seems not to be affected by increasing concentration as indicated by the unchanged general pattern of the plots, (Figure 9B). The Nyquist plots are all composed of two overlapping depressed semi-circles in the entire range of available frequency. The recognition of two time constants is further amplified through the Bode presentation, (Figure 9C). Increasing methanol concentration dramatically decreases the diameter of the low frequency semi-circle while the diameter of the high frequency semi-circle is moderately affected. Scheme 1 presents an equivalent circuit compatible with the findings where R_s, CPE_1 and R_{ct} are the solution resistance, double layer capacitance and charge transfer resistance associated with the electro-catalytic oxidation of methanol respectively. On the other hand, CPE_2 and R_f are attributable to the electrochemical characteristics of the $Ni(OH)_2$/NiOOH film. Adding methanol decreases R_{ct} which asymptotically approaches 111.3 ohm, (Figure 10). At the same time R_f drops and reflects the steady state ratio of $NiOOH/Ni(OH)_2$. The results are presented in Table 1.

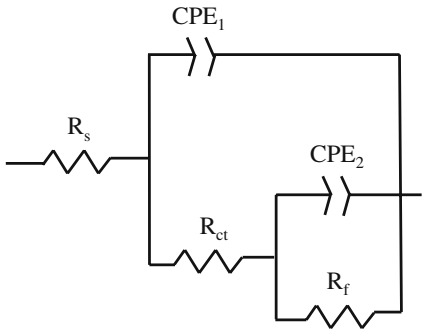

Scheme 1. Equivalent circuit compatible with the Nyquist diagrams in Fig. 9 applicable both in the presence and absence of methanol.

4. Conclusion

It is concluded that copper/nickel alloy having 40% copper is superior to pure nickel in the electro-oxidation of methanol. The specific activity of the alloy electrocatalyst signified as oxidation current density is over 10 times that of pure nickel at the same potential. The kinetic parameters of the reaction, diffusion coefficient

Table 1. Values of the elements in the equivalent circuit (Scheme 1) fitted in the Nyquist plots of Figure 9 and the corresponding relative errors (parenthesis).

R_s/Ω^{-1}	$CPE_1(\times 10^5)/\Omega^{-1}\ s^n$	n_1	R_{ct}/Ω^{-1}	$CPE_2(\times 10^4)/\Omega^{-1}\ s^n$	n_2	R_f/Ω^{-1}	C_m/M^{-1}
17.1 (0.6%)	1.16 (1.5%)	0.83 (1.0%)	316.6 (1.1%)	3.11 (1.0%)	0.89 (0.5%)	19860.3 (5.1%)	0.00
17.0 (0.2%)	2.56 (0.8%)	0.91 (0.5%)	251.9 (0.8%)	4.82 (0.5%)	0.90 (0.9%)	5535.9 (3.6%)	0.05
14.2 (0.4%)	1.91 (0.9%)	0.99 (0.9%)	190.1 (1.2%)	3.80 (1.6%)	0.90 (0.6%)	3143.0 (1.2%)	0.10
17.0 (0.2%)	3.50 (1.4%)	0.93 (0.8%)	172.7 (1.3%)	2.94 (0.8%)	0.81 (1.2%)	2051.9 (1.1%)	0.20
14.0 (0.1%)	4.00 (1.1%)	0.90 (0.3%)	151.1 (1.3%)	3.54 (0.9%)	0.90 (1.1%)	1237.0 (0.1%)	0.50
14.0 (0.1%)	2.88 (2.1%)	0.85 (0.3%)	121.0 (1.9%)	3.90 (1.4%)	0.91 (1.2%)	955.5 (1.5%)	1.00
14.0 (0.4%)	6.19 (3.4%)	0.81 (0.5%)	111.3 (0.9%)	3.19 (1.1%)	0.89 (1.6%)	329.9 (1.8%)	5.00

and rate constant, were derived through cyclic voltammetry and chronoamperometry and are 2.16×10^{-4} cm^2 s^{-1} and 1979.01 cm^3 mol^{-1} s^{-1}. An Equivalent circuit compatible with the reaction sequence was constructed on the basis of impedance measurements. The Porous nature of the catalytic layer, its changing resistance and specific activity with the concentration of methanol were confirmed through impedance studies.

Acknowledgements

Financial support of the research council of K. N. Toosi University of Technology is gratefully acknowledged. The authors also extend gratitude to Mr. M. Asgari for the skillful preparation of alloy samples.

References

1. S. Wasmus and A. Küver, *J. Electroanal. Chem.* **461** (1999) 14.
2. X. Ren, P. Zelenay, S. Thomas, J. Davey and S. Gottesfeld, *J. Power Sources* **86** (2000) 111.
3. A.N. Golikand and S.M. Golabi, *J. Power Sources* **145** (2005) 116.
4. A.N. Golikand, S. Shahrokhian, M. Asgari, M.G. Maragheh, L. Irannejad and A. Khanchi, *J. Power Sources* **144** (2005) 21.
5. M. Breiter, *Electrochim. Acta* **12** (1967) 1213.
6. M. Schell, *J. Electroanal. Chem.* **457** (1998) 221.
7. H. Nonaka and Y. Matsumura, *J. Electroanal. Chem.* **520** (2002) 101.
8. R. Parsons and T. Vander Noot, *J. Electroanal. Chem.* **257** (1988) 9.
9. M.A. Abdel Rahim, R.M. Abdel Hameed and M.W. Khalil, *J. Power Sources* **134** (2004) 160.
10. P.V. Samant and J.B. Fernandes, *J. Power Sources* **79** (1999) 114.
11. M.M.P. Janssen and J. Moolhuysen, *Electrochim. Acta.* **21** (1976) 861.
12. B. Beden, F. Kadirgan, C. Lamy and J.M. Leger, *J. Electroanal. Chem.* **142** (1982) 171.
13. G.T. Burstein, C.J. Barnett, A.R. Kucernak and K.R. Williams, *Catal. Today* **38** (1997) 425.
14. M. Jafarian, M.G. Mahjani, H. Heli, F. Gobal, H. Khajehsharifi and M.H. Hamedi, *Electrochim. Acta* **48** (2003) 3423.
15. M.L. Cubeiro and J.L.G. Fierro, *Appl. Catal.* **168** (1998) 307.
16. M. Fleischmann, K. Korinek and D. Pletcher, *J. Electroanal. Chem.* **31** (1971) 39.
17. H. Heli, M. Jafarian, M.G. Mahjani and F. Gobal, *Electrochim. Acta* **49** (2004) 4999.
18. T.R.L.C. Paixao, D. Corbo and M. Bertotti, *Anal. Chim. Acta* **472** (2002) 123.
19. K. Kano, M. Torimura, Y. Esaka, M. Goto and T. Ueda, *J. Electroanal. Chem.* **372** (1994) 137.
20. Y. Xie and C.O. Huber, *Anal. Chem.* **63** (1991) 1714.
21. L.D. Burke and K.J. O' Dwyer, *Electrochim. Acta* **36** (1991) 1937.
22. C. Fan, D.L. Piron, A. Sleb and P. Paradis, *J. Electrochem. Soc.* **141** (1994) 382.
23. T.C. Wen, C.C. Hu and Y.J. Li, *J. Electrochem. Soc.* **140** (1993) 2554.
24. A.J. Bard, R. Parsons and J. Jordan (ed.), *Standard Potentials in Aqueous Solutions* (Marcel Dekker, NewYork, 1985).
25. M. Jafarian, M.G. Mahjani, H. Heli, M. Heydarpoor and F. Gobal, *Electrochem. Commun.* **5** (2003) 184.
26. J. Taraszewska and G. Roslonek, *J. Electroanal. Chem.* **364** (1994) 209.
27. A.A. El-Shafei, *J. Electroanal. Chem.* **471** (1999) 89.
28. M.-S. Kim, T.-S. Hwang and K.-B. Kim, *J. Electrochem. Soc.* **144** (1997) 151.
29. F. Hahn, B. Beden, M.J. Croissant and C. Lamy, *Electrochim. Acta* **31** (1996) 335.
30. A. Clark, *in* The Chemisorptive Bond, Basic Concepts, Academic press, NY & London, (1974) p. 57.
31. G. Roslonek and J. Taraszewska, *J. Electroanal. Chem.* **325** (1992) 285.
32. R.-S. Schebler-Guzam, J.R. Vilche and A.J. Arvia, *Corros. Sci.* **18** (1978) 441.
33. S. Ohi, *Vapor-Liquid Equilibrium Data, Physical Science Data Series* vol. 37 (Elsevier, Amsterdam, 1989), pp. 94.
34. A.J. Bard and L.R. Faulkner Electrochemical Methods. Wiley, Chapter 12 (2001).